Effectiveness Evaluation of the Measures for Improving Resilience at Ultra-High Temperatures

Yuichi ONODA[a*], Hiroyuki NISHINO[a], Kenichi KURISAKA[a], Hidemasa YAMANO[a]
[a]Japan Atomic Energy Agency, O-arai, Japan

Abstract: This paper describes the development of measures for improving resilience of the sodium-cooled fast reactor structure using a failure mitigation technology, which suppresses the expansion of breakage or damage even if it occurs due to ultra-high temperatures exceeding design expectations, and the effectiveness evaluation of the measures. Against the accident sequence in which existing measures fail and lead to core damage, a new measure to prevent core damage have been developed by applying failure mitigation technology that is expected to be effective at ultra-high temperatures. To prevent core damage in the event of an accident progressing to an ultra-high temperature state, both measures to prevent overpressure in the reactor vessel and measures to cool the reactor core are required. As measures to prevent overpressure, two measures were selected: one is to reduce the pressure in reactor vessel by operators and the other is to install a rupture disc. As a core cooling measure, a core cooling concept was developed that promotes radiant heat transfer from the reactor vessel and cools the containment vessel outer surface by natural convection named Containment Vessel Auxiliary Cooling System (CVACS). These two measures were installed as measures for improving resilience. A method to use the reduction rate of core damage frequency as an indicator for the effectiveness of the measures for improving resilience was developed by considering the uncertainty of accident progression and the success or failure of the measures. The success probability of core cooling was evaluated by evaluating the core cooling performance using CVACS, reflecting the results of structural analysis and human reliability analysis as the effectiveness of the measures for improving resilience at ultra-high temperatures. By implementing measures for improving resilience in addition to existing measures, the core damage frequency of Japan loop-type sodium-cooled fast reactor caused by the loss of heat removal system has been reduced by two orders of magnitude of the previous level.

Keywords: SFR, LOHRS, CVACS, resilience, failure mitigation technology

1. INTRODUCTION

A failure mitigation technology is approach to improving resilience of the nuclear reactor structure [1]. This technology enables to maintain an important safety function by controlling the failure behavior of the structure by design. In this paper, the failure mitigation technology is to prevent the Reactor Vessel (RV) from collapsing/rupturing by intentionally releasing the load on the RV to the floor by contact at an ultra-high temperature, thereby avoiding the rapid leakage of sodium from the broken RV and the resultant rapid exposure of the core.

Based on previous studies of the Japan loop-type sodium-cooled fast reactor (SFR) [2] with a thermal power of 1765 MW and a homogeneous core using MOX fuel, Loss of Heat Removal Systems (LOHRS) was identified as a group of accident sequences in which measures for improving resilience could be applied in this study.

Our study to date has developed a concept for the effectiveness evaluation of the measures for improving resilience using the reduction rate in core damage frequency by the failure mitigation technology as an evaluation index [3] (see Figure 1). The event tree on the left in Figure 1 is the one in which a branching for the success or failure of the measures for improving resilience has been introduced to an existing event tree. From the figure on the left, one can recognize that core damage can be prevented by introducing measures for improving resilience for accident sequences that would lead to core damage if existing measures (Accident Management, AM) failed. The bar graph on the right plots the core damage frequency with and without the measures for improving resilience. This graph allows to show the effectiveness of measures for improving resilience to be expressed in terms of their effect on reducing core damage frequency.

In the previous study, it was clarified that the following two measures were indispensable to improve resilience at ultra-high temperature conditions: one is to recover cooling capability of the core and the other is to prevent over pressure in RV [4].

In this study, as a core cooling measure, a core cooling concept was developed that promotes radiant heat transfer from the RV and cools the containment vessel outer surface by natural convection named Containment Vessel Auxiliary Cooling System (CVACS). As measures to prevent overpressure, two measures were defined: one is to reduce the pressure in RV by operators and the other is to install a rupture disc. A method to use the reduction rate of core damage frequency as an indicator for effectiveness of the measures for improving resilience was developed by considering the uncertainty of accident progression and the success or failure of the measures.
In this paper, the concept of CVACS and its effectiveness are described in section 2, and the probability of successful core cooling was evaluated by reflecting CVACS effectiveness, the results of structural analysis and human reliability evaluation in section 3.

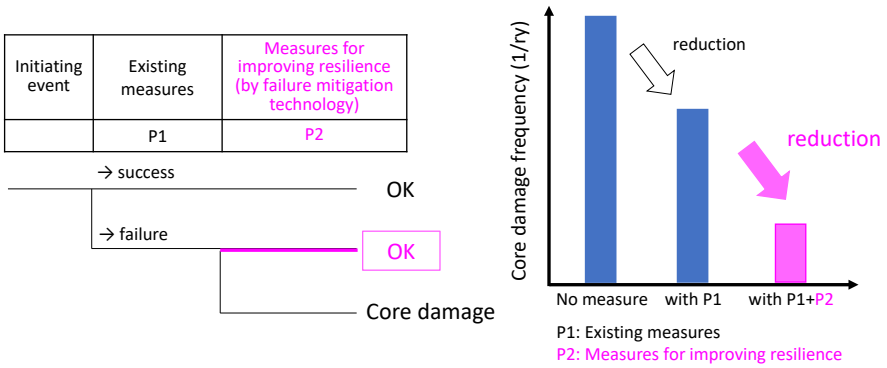

Figure 1. The concept of effectiveness evaluations for improving resilience

2. EFFECTIVENESS EVALUATION OF CVACS

2.1. The concept of CVACS

We have devised the CVACS, the concept of which is shown in Figure 2, as a measure to effectively cool the SFR core at ultra-high temperature conditions.

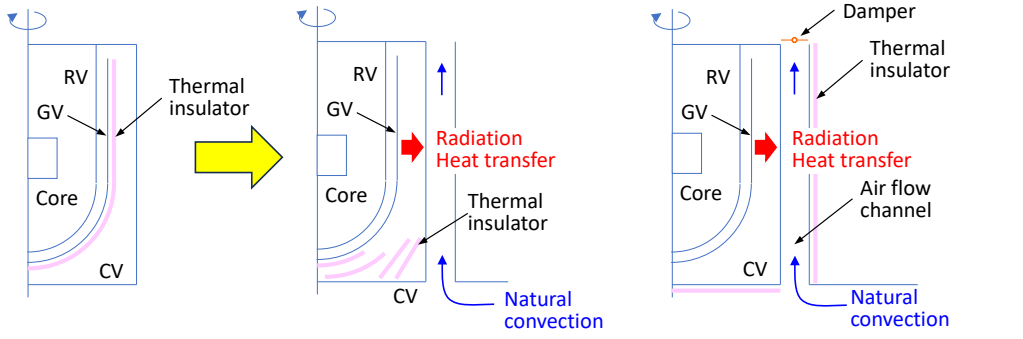

Figure 2. The concept of CV cooling by CVACS

CVACS concept (A) is a concept to remove decay heat generated in the core by removing the insulation material installed on the outer surface of the Guard Vessel (GV) as the accident progresses, transferring decay heat from the RV through the GV to the Containment Vessel (CV) by radiation heat transfer, and cooling the CV by natural convection of outside air. CVACS concept (B) is a concept to install insulation material, which is conventionally installed on the outer surface of the GV, on the outside of the air flow channel located at outer surface of the CV and to cool the CV by directing outside air into the air flow channel by natural convection. A damper is installed at the upper end of the air flow channel on the outside of the CV and is closed during normal operation. In the event of an accident, the damper is opened to promote natural convection heat transfer and cool the CV. The following section evaluates the cooling ability of the core by this CVACS.

2.2. Calculation cases

In order to understand the impact of uncertainty on CV cooling by CVACS and to develop appropriate countermeasures, the following evaluation cases are set up and the cooling performance of CVACS is evaluated.

Case 1 Basic case using CVACS concept (A) having thermal insulator outside the GV and removing it depending on the accident progression. Uncertainty distributions are assumed to be uniform for the following parameters: 1) activation time of CVACS, 2) insulation removal height, and 3) emissivity of GV and CV.
Case 2 Uncertainty distribution of emissivity in Case 1 is replaced with the one in which frequency of the emissivity take the maximum value at 0.7 (see Figure 6).
Case 3 Uncertainty distribution of insulation removal height is replaced with the one in which frequency of insulation removal height take the maximum value at 20 m (see Figure 6).
Case 4 Improved case using CVACS concept (B) having thermal insulator outside the air flow channel and controlling air flow by opening damper. Uncertainty distribution of emissivity in which frequency of the emissivity take the maximum value at 0.7 (see Figure 6) is applied.

Cases 1 to 3 are cases using the CVACS concept (A), and case 4 is a case using the CVACS concept (B). Case 1 is a basic case using CVACS concept (A). Case 4 is an improved case using CVACS concept (B). Cooling performance improves in the order of cases 1 to 4.

2.3. Calculation method

The cooling performance of CVACS is evaluated by using a steady one-dimensional heat transport equation taking the chimney effect into account. The concept of the evaluation is shown on Figure 3. When taking the chimney effect into account, the outside air velocity (and the heat transfer coefficient that depends on it) is a function of the CV temperature (chimney outlet temperature), so a solution is obtained by performing a convergence calculation with the CV temperature as a parameter.

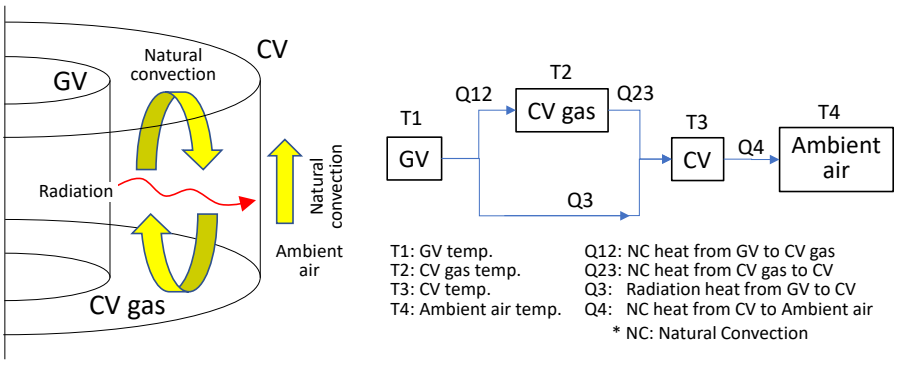

(a) The concept of calculation model considering radiation and natural convection heat transfer from GV to the ambient air

(b) Heat transport path

Figure 3. The concept of evaluation method for coolability of CVACS

The GV temperature T1, which is the boundary condition on the heat generation side, is given as the result of the plant dynamics analysis of the LOHRS accident sequence in which the cooling of the core fails. The time evolution in the reactor outlet coolant temperature during LOHRS of Japan loop-type SFR and the approximate decay heat level are shown in Table 1 [5]. The ambient air temperature T4, which is the boundary condition, is set to 20°C.

Table 1. Decay heat and coolant temperature at RV outlet at representative time

Time after LOHRS initiation (h)	Decay heat (MW)	Coolant temperature (°C)
7	15	700
12	13	800
18	12	900

The evaluation procedure is as follows: First, the amount of heat transferred from the GV to the CV (radiation + natural convection in the CV), f, is defined using the CV temperature as a parameter, as follows:

$$f = Q_{12} + Q_3 \tag{1}$$

where Q_{12} is the natural convection heat from GV to CV gas, and Q_3 is the radiation heat from GV to CV. Q_3 can be obtained by radiation heat transfer equation,

$$Q_3 = A_1 F_{13} \sigma (T_1^4 - T_3^4) \tag{2}$$

$$\frac{1}{F_{13}} = \frac{1}{e_1} + \frac{A_1}{A_3}\left(\frac{1}{e_3} - 1\right) \tag{3}$$

where F_{13} is radiation form factor, σ is the Stefan–Boltzmann constant, T_1 and T_3 are the temperature of GV and CV, e_1 and e_3 are the emissivity of GV and CV, and A_1 and A_3 are the surface area for radiation heat transfer of GV and CV, respectively. Q_{12} is obtained by using the relation $Q_{12} = Q_{23}$ and subtracting T_2 from equations (4) and (5),

$$Q_{12} = A_1 h_{12,f,av} (T_1 - T_2) \tag{4}$$

$$Q_{23} = A_3 h_{23,f,av} (T_2 - T_3) \tag{5}$$

where $h_{12,f,av}$ and $h_{23,f,av}$ are average natural convection heat transfer coefficient of GV surface and CV surface, and T_2 is the temperature of CV gas, respectively. $h_{12,f,av}$ is given using the formulation of natural convection heat transfer of gas at vertical plate [6] as follows:

$$h_{12,f,av} = \frac{k_{N2}}{L_{GV}} Nu_{12,av} \tag{6}$$

$$Nu_{12,av} = \left(\frac{Pr_{12}}{2.4+4.9\sqrt{Pr_{12}}+5Pr_{12}}\right)^{0.25} Pr_{12} \left(\frac{\nu_2}{\nu_1}\right)^{0.21} (Gr_{12} Pr_{12})^{0.25} \tag{7}$$

where k_{N2} is thermal conductivity of CV gas (Nitrogen), L_{GV} is the height of GV, $Nu_{12,av}$ is average Nusselt number, Pr_{12} and Gr_{12} are Plandtl number and Grashoff number, ν_1 and ν_2 are kinematic viscosity of CV gas at GV surface and bulk Nitrogen gas in the CV, respectively. The temperature dependency of physical properties of Nitrogen gas in the CV is considered in the calculation using film temperature T_{f12}, as follows:

$$T_{f12} = \frac{T_1 + T_2}{2} \tag{8}$$

The average natural convection heat transfer coefficient of CV surface, $h_{23,f,av}$, is also calculated in the same manner using equations (6) to (8). Then, correlation g is defined for calculating the heat transfer from the CV to the air taking the chimney effect into account using the forced convection heat transfer at vertical plate [6], with the CV temperature as a parameter, as follows:

$$g = Q_4 = A_3 h_{CV,f,av} (T_3 - T_4) \tag{9}$$

$$h_{CV,f,av} = \frac{k_{air}}{L_{CV}} \cdot 0.037 \cdot {Re_{34}}^{0.8} \cdot {Pr_{34}}^{1/3} \tag{10}$$

where k_{air} is the thermal conductivity of air, L_{CV} is the height of CV, Re_{34} and Pr_{34}, are Reynolds number and Plandtl number of the air, respectively. T_4 is the inlet temperature of the air. The temperature dependency of physical properties of air in the air flow channel is considered in the calculation of them using average temperature T_{f34}, as follows:

$$T_{f34} = \frac{T_{out} + T_{in}}{2} \tag{11}$$

where T_{in} and T_{out} are the inlet and outlet temperature of the air, respectively. Velocity of air, u_{air}, is given by the equation of chimney effect, as follows:

$$u_{air} = C\sqrt{2gh_{chan}\frac{T_{out} - T_{in}}{T_{in}}} \tag{12}$$

where C is the air intake constant (C is set to 0.7), g is the gravitational acceleration, and h_{chan} is the height of the air flow channel. T_{in} and T_{out} have another relation by temperature increase of air due to natural convection heat flow:

$$T_{out} = \frac{Q_4}{\rho_{air} A_z u_{air} {Cp}_{air}} + T_{in} \tag{13}$$

where A_z is the flow area of air flow channel. Subtracting T_{out} of eq. (13) into eq. (12), the relation between u_{air} and $T_{in} = T_4$ is obtained, and then g is obtained as a function of CV temperature T_3. Then, CV temperature is obtained using the relation $f = g$. In this evaluation, since it was difficult to solve $f = g$ analytically, it was solved numerically using equations (1) and (6).

2.4. Calculation results

The cooling performance of CVACS was evaluated under the following 216 conditions with GV and CV diameter being 12 m and 40 m, their heights being 20 m, and chimney height being 20 m, respectively:

a) GV temperature: 3 levels with 700, 800, and 900°C as representative temperatures
b) Emissivity: 9 levels in 0.1 increments (0.1 to 0.9)
c) Insulation removal height: 8 levels of 1, 2, 3, 5, 7, 10, 15, and 20 m

Calculation results of the heat removal capability of CVACS is shown on Figure 4 against the insulation removal height and emissivity.

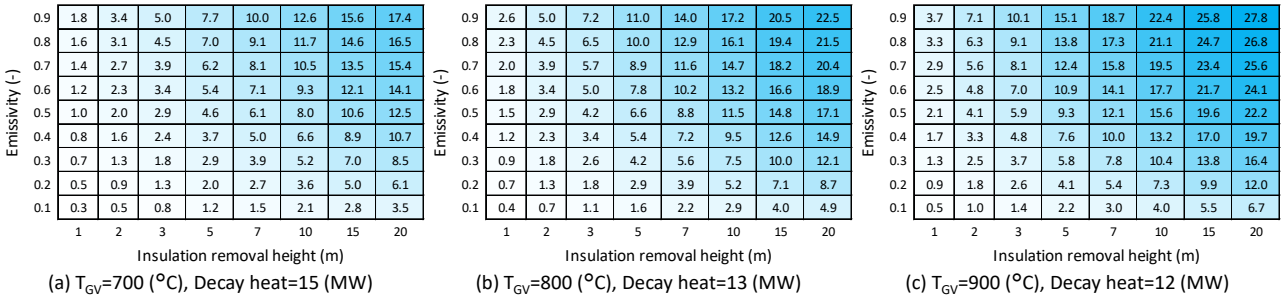

Figure 4. Result of heat removal capability (W) of the CVACS at each GV temperature

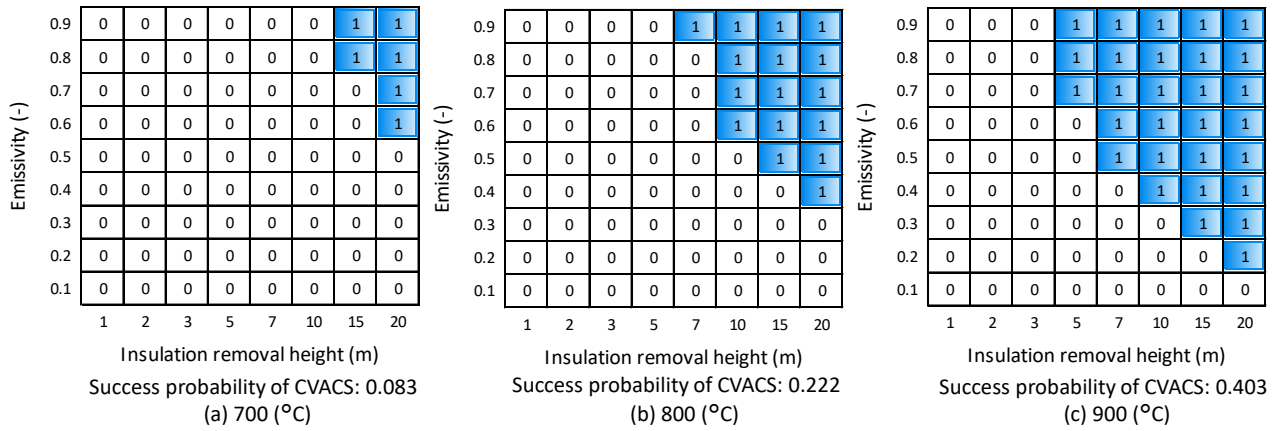

Figure 5. Success condition of cooling by CVACS at each GV temperature (Case 1)

The larger the emissivity and the higher the insulation removal height, the larger the amount of heat removal. Using these results, the CVACS cooling performance under the conditions of cases 1 to 4 is evaluated. Figure 5 shows the results of the evaluation of the success or failure of cooling in case 1. Like Figure 4, Figure 5 shows the success or failure of cooling with respect to the insulation removal height and emissivity. Here, cooling is judged to be successful when the amount of heat removed by CVACS at a certain time (represented by the coolant temperature) exceeds the decay heat. From Figure 5, if the occurrence probability of all levels of CVACS operating temperature (time), emissivity, and insulation removal height is uniformly distributed, the conditional probability of cooling success is 0.236.

Next, we changed the uncertainty distribution of emissivity. In Case 2, such uncertainty distribution of emissivity was applied that has a normal distribution with a mean value of 0.7 and a standard deviation of 0.07 being discretized with a width of 0.1 and the upper and lower ends being cut off (see Figure 6(a)), based on the literature [7] in which the emissivity was evaluated to be about 0.7. In this case, the uncertainty distribution of the CVACS operating temperature is uniform, but the conditional probability of cooling success increases to 0.375 compared to 0.236 in Case 1.

Next, an evaluation was performed on the Case 3 in which the uncertainty distribution of the CVACS insulation removal height was changed from Case 2. Figure 6(b) shows an uncertainty distribution, in which higher insulation removal heights have a higher frequency. In this case, the uncertainty distribution of the CVACS operating temperature is uniform, but the conditional probability of cooling success is 0.593, which is higher than 0.375 in Case 2.

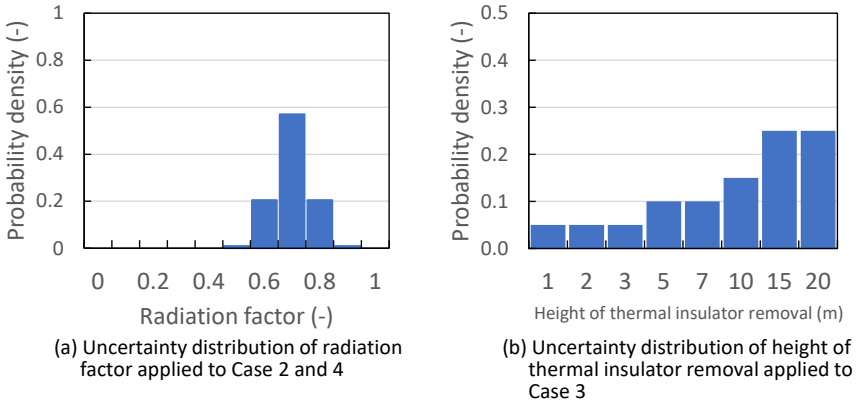

Figure 6. Uncertainty distribution of (a) radiation factor applied to Case 2 and 4 and (b) height of thermal insulator removal applied to Case 3

Next, an evaluation was performed on the Case 4 where the insulation is installed on the outside of the CV and a damper is installed at the outlet of the cooling channel. In Case 4, the insulation is installed on the outside of the CV from the initiation of the accident, so the amount of heat removal corresponds to the case where the insulation removal height is 20 m. In addition, since the same emissivity uncertainty as in Case 2 is applied, the cooling conditions in this case correspond to the emissivity range from 0.5 to 0.9 for the column with an insulation removal height of 20 m in Figure 4, and the conditional probability of cooling success at each temperature is 0.994 (700°C), 1.0 (800°C), and 1.0 (900°C), totaling 0.998.
However, even if cooling fails at 700°C (heat removal amount < decay heat), the GV temperature will rise due to insufficient heat removal over time and the decay heat will decay. If this is taken into account when judging coolability, even under conditions where cooling is judged to have failed at 700°C, the coolant temperature will rise over time, and the increasing heat removal capacity will exceed the decay heat that is decaying, resulting in successful cooling. In other words, this is equivalent to eliminating the assumption that the uncertainty regarding the CVACS activation time is uniform and considering the balance between heat generation and heat removal depending on the accident progression. If this is taken into account for Case 4, the conditional probability of successful cooling is 1.0 (cooling will always be successful). The evaluation results of the success probability for Cases 1 to 4 are shown in Table 2.

Table 2. Success probability of CVACS at each GV temperature

ID	**700** °C	**800** °C	**900** °C	**Total**
Case 1	0.083	0.222	0.403	0.236
Case 2	0.151	0.375	0.598	0.375
Case 3	0.302	0.650	0.829	0.593
Case 4	0.994	1.0	1.0	1.0*1

*1 Probability considering dependency of success criteria to the accident progression. This results in the probability at 900 °C.

3. EVALUATION OF CORE DAMAGE FREQUENCY

To quantify the effectiveness of the measures for improving resilience, it is necessary to quantify the event tree heading P2 shown in Figure 1. Here, we decided to evaluate the branching probability of heading P2 using a decomposition event tree. From the previous studies, it was found that the following elements are necessary to improve resilience: depressurization inside the RV and restoration of coolability. The results of a structural response analysis under high temperature conditions assuming LOHRS [8] showed that depressurization inside the RV is necessary to ensure the integrity of the RV boundary. There are two methods for depressurizing the RV: one is by operator operation, and the other is passive depressurization using a rupture disk. In addition to

the probability of successful cooling by CVACS, the success probability of these methods must be evaluated. Below, we will describe these evaluation methods and their results.

3.1. Information from structural calculations

Structural analyses were carried out to evaluate the integrity of the reactor coolant boundary at ultra-high temperature conditions [8]. The findings obtained from this are as follows:

a) Even if a very high temperature state is reached, the primary system boundary function required for cooling will be maintained if attention is paid to the structure supporting the RV and GV, and the RV is successfully depressurized before the sodium temperature reaches 900°C, or depressurization is successful due to rupture of the rupture disk.
b) If the operator's depressurization operation fails but the depressurization by the safety valve is successful (0.8 MPa is maintained), and depressurization cannot be achieved before the sodium temperature reaches 900°C after the event occurs, the primary system boundary function required for cooling will be lost approximately 20 hours after the event occurs.
c) If the operator's depressurization operation and the depressurization by the safety valve fail, and the rupture disk does not work, the primary system boundary function required for cooling will be lost approximately 12 hours after the event occurs.

These findings will be reflected in the evaluation of the effectiveness of measures for improve resilience.

3.2. Quantification of the event tree

A decomposition event tree was constructed by reflecting the findings from the CVACS cooling evaluation and the structural analyses. The decomposition event trees constructed for cases 1 to 3 and for case 4 are shown in Figures 7 and 8, respectively. The definitions of each heading A to G and the branching probabilities set are shown in Table 3.

This decomposition event tree (Figure. 7) has four headings (A, B, D and F) that indicates the success or failure of the operator's recognition or operation. The success probability of these headings was evaluated using the THERP method, which is one of the human reliability evaluation methods, assuming a shift consisting of three six-person operator teams. The probability that the equipment does not operate as expected was set to 1E-3 uniformly. The uncertainty of the CVACS operation time (heading F) was set to 1E-3 as the probability that it does not operate as expected, and if it operates as expected, it was divided equally by the number of time intervals (number of temperature intervals). The probability of successful cooling by CVACS (heading G) was the total probability of successful cooling by CVACS for each case shown in Table 2. As a result of quantifying the decomposition event tree on Figure 7, the probability of successful cooling in cases 1 to 3 was evaluated to be 0.236, 0.375, and 0.594, respectively (see Table 4). For Case 4, the probability of operator recognition and operation success or failure, and the probability of the equipment not operating as expected were set in the same way as for Cases 1 to 3. In Case 4, cooling by CVACS was always successful regardless of time, so the branching of CVACS coolability (heading G) differed from the other cases, and the conditional probability of cooling success (heading F') was evaluated as 0.995.

The branching probability obtained by quantifying the decomposition event tree was applied to the heading P2 of event tree in Figure 1 to quantify the core damage frequency for all accident sequences that are caused by internal events which lead to LOHRS in the Japan loop-type SFR. Figure 9 shows the quantification result of the simplified event tree when the initiating event is Loss of offsite power (Case 4). The same operation was applied to all the 21 internal initiating events leading to LOHRS in the Japan loop-type SFR [3] applying the branching probability of Cases 1 to 4 to the success probability of the measures for improving resilience, and then core damage frequencies of Cases 1 to 4 were obtained as shown on Figure 10. Figure 10 also shows the case where the success probability of the measures for improving resilience is zero (No measure). It can be seen from Figure 10 that the core damage frequency is reduced in the order of Cases 1 to 4 compared to the case without measures for improving resilience. By taking measures for improving resilience in addition to the existing measures, the core damage frequency was reduced from 3.9×10^{-8} (1/reactor-year, without measures for improving resilience) to 2.7×10^{-10} (1/reactor-year, Case 4).

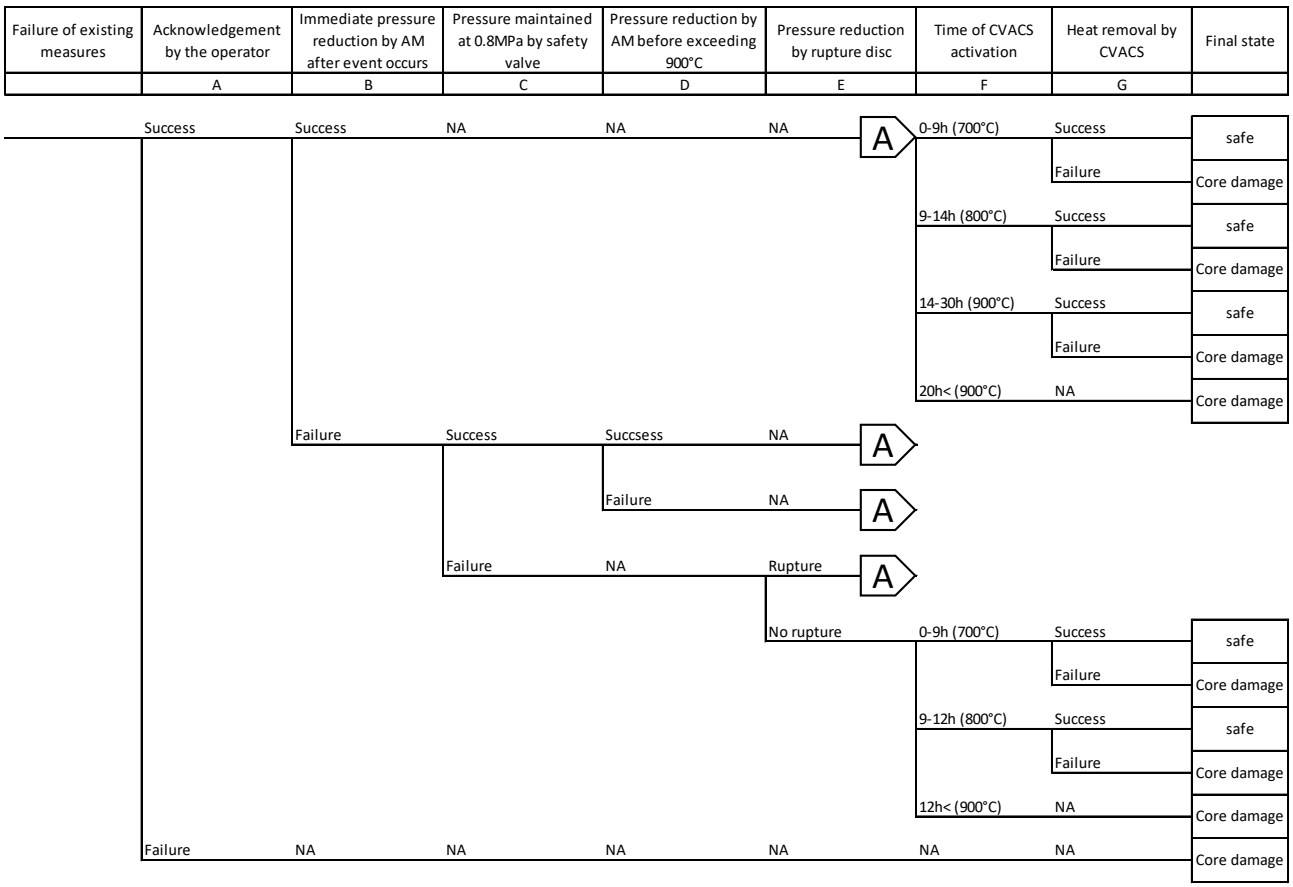

Figure 7. Decomposition event tree for the heading "Success of the measures for improving resilience" in the simplified event tree (for Case 1, 2 and 3)

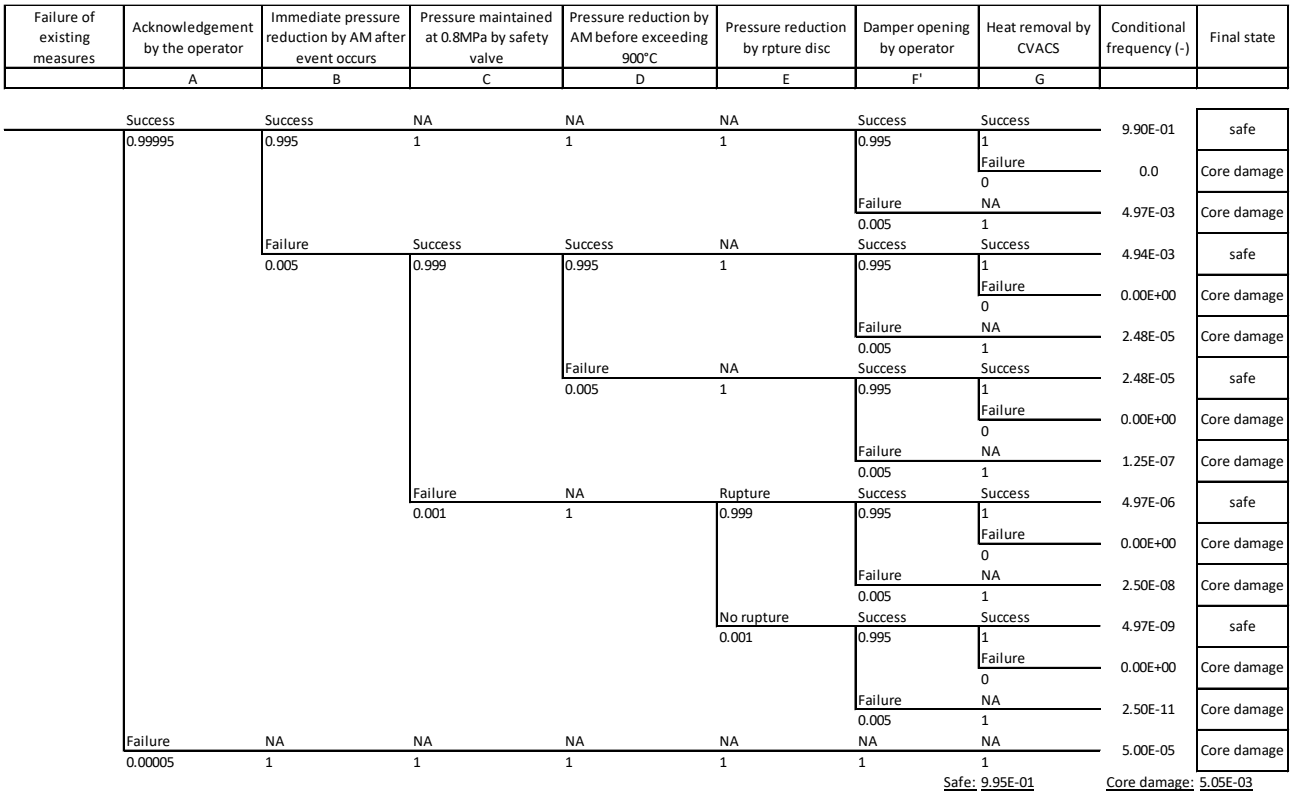

Figure 8. Decomposition event tree for the heading "Success of the measures for improving resilience" in the simplified event tree (for Case 4)

Table 3. Definition of each heading and set branching probability

ID	Heading name	Definition	Set branching probability
A	Acknowledgement by the operator	Distinguish whether the operator recognizes the occurrence of an abnormality	Failure frequency: 5.0E-5
B	Immediate pressure reduction by AM after event occurs	Distinguish the success or failure of AM measures taken by operators to reduce pressure after an event occurs	Failure frequency: 5.0E-3
C	Pressure maintained at 0.8MPa by safety valve	Distinguish whether the safety valve maintains the expected pressure	Failure frequency: 1.0E-3
D	Pressure reduction by AM before exceeding 900°C	Distinguish whether the AM measures taken by operators to reduce pressure before the primary coolant temperature reached 900°C were successful or not	Failure frequency: 5.0E-3
E	Pressure reduction by rupture disc	Distinguish between success and failure of decompression due to rupture of rupture disk	Failure frequency: 1.0E-3
F	Time of CVACS activation (Case 1 to 3)	Distinguish whether CVACS is working as expected or not	Failure frequency: 1.0E-3 Uniform distribution in time if CVACS is activated as expected.
F'	Damper opening operation by operator (Case 4)	Distinguish between success and failure of damper opening operation by operator	Failure frequency: 5.0E-3
G	Heat removal by CVACS	Distinguish between successful and failure of cooling by CVACS	Depending on calculation case

Loss of offsite power	Existing measures	Measures for improving resilience (Measures A* and B**)	Occurrence Frequency (1/ry)	Final state
IP	P1	P2		
1.50E-02 (1/ry)	Success 1-6.67E-07		1.50E-02	Safe
	Failure 6.67E-07	Success 9.95E-01	9.95E-09	Safe
		Failure 5.00E-03	5.00E-11	Core damage

A* Measure to keep coolant inside the primary boundary by avoiding opening failure on RV if it is vertically extended by its weight when primary coolant temperature increases high (measure using the failure mitigation technology).

B** Measures to prevent core damage other than A: one is the additional heat transport system which can operate under ultra-high temperature condition, the other is the system which depressurize primary system and collects and contains the sodium vapor.

Figure 9. Simplified event tree for Japan loop type SFR (LOHRS, Case 4)

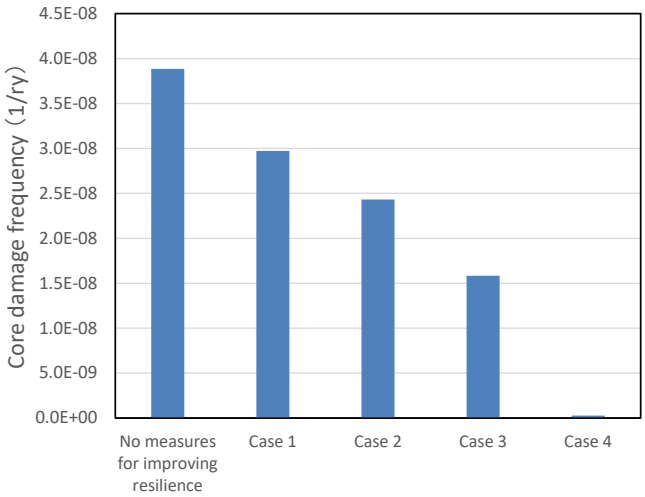

Figure 10. Evaluation result of core damage frequency for each calculation case and in case of "no measures for improving resilience"

Table 4. Evaluation results of decomposition event tree for Case 1 to 4

ID	Case 1	Case 2	Case 3	Case 4
Success	0.236	0.375	0.594	0.995
Failure	0.764	0.625	0.406	0.005

4. CONCLUSION

In this study, the effectiveness of resilience improvement measures by the failure mitigation technology was quantitatively evaluated for accident sequences that lead to extremely high temperatures in the loop-type SFR. The measures to improve resilience at extremely high temperatures are overpressure prevention measures (depressurization by operators and installation of rupture disks) and core cooling measures by cooling the CVACS, which were described in the event tree with examining the uncertainty of accident progression and the success or failure of resilience improvement measures. This study evaluated the coolability of the core using CVACS, serving for the success probability of core cooling. The probability was evaluated by reflecting the results of structural analysis and human reliability evaluation as well. The quantification of the branching probability of the event tree allows us to evaluate the effectiveness of measures to improve resilience against extremely high temperatures. By implementing resilience improvement measures that employ failure mitigation technology in addition to existing measures, the frequency of core damage caused by LOHRS was reduced by two orders of magnitude of the previous level.

Acknowledgements

This work was supported by Ministry of Education, Sports, Science and Technology (MEXT) under Innovative Nuclear Research and Development Program Grant Number JPMXD0220353828.

References

[1] Kasahara, N., Wakai, T., Nakamura, I. and Sato, T., “Application of fracture control to mitigate failure consequence under BDBE,” Proceeding of the ASME 2020 Pressure Vessels & Piping Conference PVP2020.
[2] Kamide, H., Ando, M., Ito, T., “JSFR Design Progress Related to Development of Safety Design Criteria for Generation IV Sodium-Cooled Fast Reactor,” Proceedings of the International Conference on Nuclear Engineering (ICONE23), Chiba, Japan, May 17-21, 2015.
[3] Y. Onoda, et. al., Development of Effectiveness Evaluations Technology of the Measures for Improving Resilience of Nuclear Structures at Ultra High Temperature, Proceedings of the Asian Symposium on Risk Assessment and Management (ASRAM2021), Virtual, October 24-27, 2021.
[4] Y. Onoda, et. al., Effectiveness Evaluation Methodology of the Measures for Improving Resilience of Nuclear Structures at Ultra-High Temperature, Proceedings of the 30th International Conference on Nuclear Engineering (ICONE30), Kyoto, Japan, May 21-26, 2023.
[5] Matsuo, E., Watanabe, M., Yamada, Y., et.al., Study on event progression in PLOHS for JSFR (1) Numerical simulation of plant dynamics phase in PLOHS, Transactions of the AESJ fall meeting (2012) Paper No. M05.
[6] JSME Data Book: Heat Transfer 5th Edition, The Japan Society of Mechanical Engineers, 2009.
[7] D. Lisowski, et. al., Technical Letter Report: An Overview of Non-LWR Vessel Cooling Systems for Passive Decay Heat Removal, Final report, ANL/NSE-21/3, Argonne National Laboratory, May, 2021.
[8] S. Futagami, et. al., Development of Failure Mitigation Technologies for Improving Resilience of Nuclear Structures (5) Resilience Improvements of Fast Reactors by Failure Mitigation for Beyond Design high Temperature Accidents, Transactions of the SMiRT 27, Yokohama, Japan, March 3-8, 2024.